Copyright © 2007 ICCES ICCES, vol.4, no.2, pp.73-80, 2007

Stress distribution due to inclined line loads in fibrous polymer composites

S. Gururaja[1] and M. Ramulu[2]

Summary

Uni-Directional Fiber-Reinforced Plastic (UD-FRP) laminates have been modeled as a quasi-homogeneous monoclinic half-space subjected to an inclined load at the surface. Complete closed form stress-fields derived previously [1] based on Lekhtinskii's formulation [2] in conjunction with the principle of analytical continuation [3] were used to study the stress-response in relation to a few parameters identified, namely, fiber-orientation, load inclination angle and spatial coordinates with respect to line load application position in the half-space domain.

Introduction

Due to the extensive use of fibrous composite as load-bearing components in recent times, there has been a renewed interest in the anisotropic half-space problem as an idealized descriptive model for analyzing UD-FRP laminates [4, 5]. Anisotropic half-space problem with surface load acting is a classical elasticity problem that has received widespread treatment by researchers in the last several decades [6]. Complete closed-form stress-fields for a line-load of fixed width acting symmetrical about the origin at the surface of an anisotropic (monoclinic) elastic half-space have been derived in [1]. The present work deals with understanding the stress-fields by conducting a parametrical analysis vis-à-vis fiber-orientation, load inclination angle and spatial coordinates with respect to the line-load application position for a given width of line load in the half-space domain. The stress-fields thus generated are believed to throw light on the edge-trimming process of UD-FRP laminates.

Inclined load problem

UD-FRP composite laminate is modeled as a continuous quasi-homogeneous linear elastic monoclinic half-space with symmetry existing about z, $X_3= 0$ axis whose stiffness properties have been calculated from standard tensor transformation relations. A Cartesian coordinate system is defined such that the angle between problem X-axis and the material X_1-axis in the anti-clockwise direction represents the fiber angle of the UD-FRP as shown in Figure 1. Based on the need to simplify the mathematical analysis, the following three assumptions have been made to derive the stress field equations [1]:- a) Generalized plane strain deformation; b) UD-FRP laminate is a continuous quasi-homogeneous linear elastic monoclinic half space; and c) Quasi-static loading scenario is considered.

[1]Graduate Student, Mechanical Engineering, University of Washington, Seattle, WA. 98195, USA
[2]Professor, Mechanical Engineering, University of Washington, Seattle, WA. 98195, USA

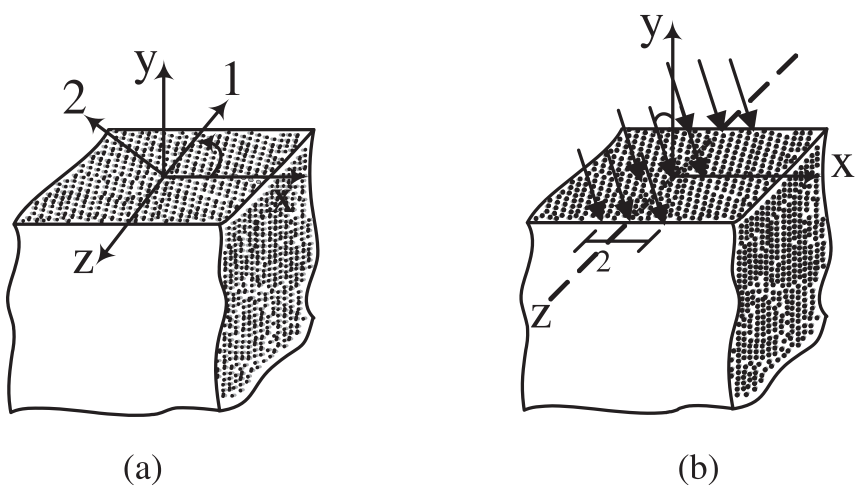

Figure 1: UD-FRP composite representation as a quasi-homogeneous continuous anisotropic elastic half-space; (a) Cartesian coordinate definition; and (b) line load with uniform magnitude along z – axis.

Stress-fields derivation

From Cauchy-Reinmann relations for analytic functions, for a function $f(z = x+iy)$ analytic in the lower half-plane $y \leq 0$, continuous up to the boundary with $f(\infty) = 0$ with ξ, a point on the boundary (abscissa):

$$\frac{1}{2\pi}\int_{-\infty}^{\infty}\frac{f(\xi)}{\xi - z}d\xi = -f(z), \quad \frac{1}{2\pi}\int_{-\infty}^{\infty}\frac{\overline{f(\xi)}}{\xi - z}d\xi = 0 \tag{1}$$

where $\bar{f}$ denotes the complex conjugate of f. This property has been used in the development of the complex potentials which are critical in the determination of stress fields.

For a half-space problem with normal and tangential components of the external tractions on the boundary $y = 0$ are denoted by $N(\xi)$ and $T(\xi)$ respectively. The boundary conditions when $y = 0$ take the form $\sigma_{yy} = N(\xi)$, $\tau_{xy} = T(\xi)$, $\tau_{yz} = 0$. From Muskhelishvelli's approach of analytic continuation (extension of Equation (1)), the complex stress functions for a monoclinic material are given by Lekhnitskii [2]: -

$$
\begin{aligned}
\Phi_1'(z_1) &= \frac{1}{2\pi i(\mu_1-\mu_2)}\int_{-\infty}^{\infty}\frac{N(\xi)\,\mu_2+T(\xi)}{\xi-z_1}d\xi \\
\Phi_2'(z_2) &= -\frac{1}{2\pi i(\mu_1-\mu_2)}\int_{-\infty}^{\infty}\frac{N(\xi)\,\mu_1+T(\xi)}{\xi-z_2}d\xi \qquad (2)\\
\Phi_3'(z_3) &= 0; \quad z_1 = x+\mu_1 y; \quad z_2 = x+\mu_2 y
\end{aligned}
$$

where μ_1, μ_2 are the eigenvalues, derived from the stiffness matrix of the half-space [1]. The corresponding stresses are thus known and computed as: -

$$
\begin{aligned}
\sigma_{xx} &= 2Re\left[\mu_1^2\Phi_1'(z_1)+\mu_2^2\Phi_2'(z_2)\right]\\
\sigma_{yy} &= 2Re\left[\Phi_1'(z_1)+\Phi_2'(z_2)\right]\\
\sigma_{zz} &= -\frac{1}{a_{33}}(a_{13}\sigma_{xx}+a_{23}\sigma_{yy}+a_{63}\tau_{xy}) \qquad (3)\\
\tau_{xy} &= -2Re\left[\mu_1\Phi_1'(z_1)+\mu_2\Phi_2'(z_2)\right]\\
\tau_{xz} &= \tau_{yz} = 0
\end{aligned}
$$

For a line load of width 2ε(x-direction) of constant magnitude N per unit length symmetric about the z-axis acting at an inclination of α with respect to the y-axis in counter-clockwise direction (Figure 1 (b)), the normal component $N(\xi) = \frac{-N\cos\alpha}{2\varepsilon}(u(\xi+\varepsilon)-u(\xi-\varepsilon))$, and the transverse component $T(\xi) = \frac{-N\sin\alpha}{2\varepsilon}(u(\xi+\varepsilon)-u(\xi-\varepsilon))$, where $u(\xi-\varepsilon)$ is the Heaviside function indicating the location of the line load compressive stresses are taken to be negative. Performing the integrations of (2), the complex stress functions are represented by

$$
\begin{aligned}
\Phi_1'(z_1) &= \frac{N(\mu_2\cos\alpha+\sin\alpha)}{4\varepsilon\pi i(\mu_1-\mu_2)}Ln\left(\frac{z_1-\varepsilon}{z_1+\varepsilon}\right),\\
\Phi_2'(z_2) &= \frac{-N(\mu_1\cos\alpha+\sin\alpha)}{4\varepsilon\pi i(\mu_1-\mu_2)}Ln\left(\frac{z_2-\varepsilon}{z_2+\varepsilon}\right) \qquad (4)\\
\Phi_3'(z_3) &= 0
\end{aligned}
$$

which reduce to Flamant's solution for an isotropic half space as demonstrated in [1]. The complete closed-form stress-field expressions are thus obtained by substituting Equation (4) in (3). It should be noted that there exists a mathematical singularity at ($\pm\varepsilon$, 0) due to the assumed discontinuous geometry of the line load. This is circumvented by considering stress-fields sufficiently away from the singularity zone.

Stress-Analysis Example

UD-FRP Graphite/Epoxy (Gr/Ep) laminate with E_{11} = 160.65 GPa, E_{22} = 9.62 GPa, E_{33} = 9.62 GPa, G_{12} = 6.32 GPa, G_{13} = 6.32 GPa, $G23$ = 3.58 GPa, ν_{12} = 0.2965, ν_{13} = 0.2965 and ν_{23} = 0.342 has been used in the present investigation. Based on the stress fields derived, a few variables have been identified to perform a parametric analysis, namely (1) Fiber-orientation θ of the UD-FRP laminate; (2) magnitude of load N acting on the UD-FRP laminate; (3) the angle α that the load makes with the vertical axis; and (4) magnitude of width 2ε of the line load. Fiber orientation θ has been identified as the most significant parameter. To this end, the variation of stress-fields with respect to fiber-orientation has been discussed in detail. For the sake of conceptual understanding, the magnitude of N has been set to unity to facilitate comparisons among the various cases. Additionally, the stresses are evaluated at locations in $x-y$ space representative of non-integer multiples of half-width of load profile ε. C.W. Liu's [7] erstwhile work of 1950 provides the basis for the present analysis.

The stress distributions σ_{xx}, σ_{yy} and τ_{xy} at various depths due to a constant line load profile of width 20 μm have been plotted for 0°, 45°, 90° and 135° fiber-orientation in Figures 2 through 6 respectively. α = 45° loading scenario as a combination effect of 0° and 90° cases has been looked at. The x- and y- coordinates are normalized with respect to the half-width of line load profile ε. Strictly speaking, as in [7], the magnitude of α would depend on the friction coefficient and the specific problem at hand. However, in this investigation the α's are chosen arbitrarily in order to characterize the behavior of stress fields, and only one case has been enumerated for brevity.

σ_{yy} distribution evolution for $\alpha = 0^{o}$ has been enumerated in figure 2. The stress fields are found to be symmetric about $x/\varepsilon = 0$ with the maximum stress magnitude occurring at $x/\varepsilon = 0$ for 0° and 90° fiber orientations. Also σ_{yy} is found to decrease more rapidly with increased depth (y/ε) for $\theta = 0^{o}$s compared to $\theta = 0^{o}$. This can be attributed to the fact that for $\theta = 0^{o}$, the fibers are aligned along the direction of the load application therefore load transfer is not as effective as in $\theta = 0^{o}$. The "fiber" phase is the load carrying member and the "matrix" phase is the load-transferring member of any composite system. This rationale explains some of the salient stress-fields characteristics enumerated in this paper. If the load acts along the direction of the fibers, the stress-dispersion would be minimal. Conversely, if the load is acting perpendicular to the fibers (or along the matrix so to speak) the stress-dispersion would be maximal. Here stress-dispersion indicates how fast the stress magnitudes decrease or decay. For example, σ_{yy} distribution for $\theta = 0^{o}$ exhibits higher stress-dispersion as compared with σ_{yy} distribution for $\theta = 90^{o}$. Another thing to note here is the fact that σ_{yy} has been specified at the

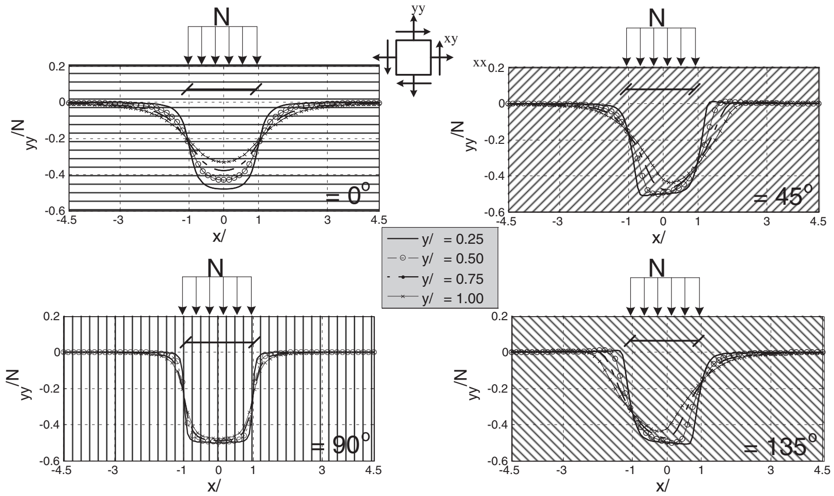

Figure 2: Variation of σ_{yy} due to line load distributions on a width 2ε of 20 µm with respect to x/ε for Normal Load Case (α = 0°).

boundary $y = 0$. Therefore, when we look at the σ_{yy} distribution across the depth, the stress-dispersion becomes an important parameter. For $\theta = 45^o$ and 135^o, the maximum occurs approximately along the direction of the fiber orientation and the stress-fields are no longer symmetric, however, they seem to be mirror images. Also interesting to note is that the stress fields for $\theta = 45^o$ and 135^o are indicative of the respective fiber orientations. This observation highlights the preservation of inherent stiffness characteristics along the respective fiber direction of an UD-FRP laminate despite the quasi-homogeneous assumption postulated during problem formulation thereby revalidating the model. Similar inferences have been drawn for σ_{yy} distribution for $\alpha = 90^o$ and have therefore not been included here.

Figure 3 depicts σ_{yy} distribution for $\alpha = 45^o$ or the combination load case. Being in the domain of linear elasticity, we would expect the stresses for the combination load case to be a sum of the $\alpha = 0^o$ and 90^o cases. Figure 4 demonstrates such an addition of stress-fields for $\theta = 0^o$ laminate under the application of horizontal and normal load cases to replicate the results for the combination load case. Such an addition of stress-fields would be valid for all fiber-orientations and can be demonstrated as for $\theta = 0^o$ laminate. Due to such a superposition, the stress-fields do not exhibit the symmetry as observed for normal and horizontal cases. We see that while both compressive and tensile stresses exist for 90°/135° laminates, only compressive stresses exist for 0°/45° laminates.

σ_{xx} distribution for combined load case has been shown in Figure 5. The additive effects demonstrated for σ_{yy} distribution in Figure 4 hold true here as well.

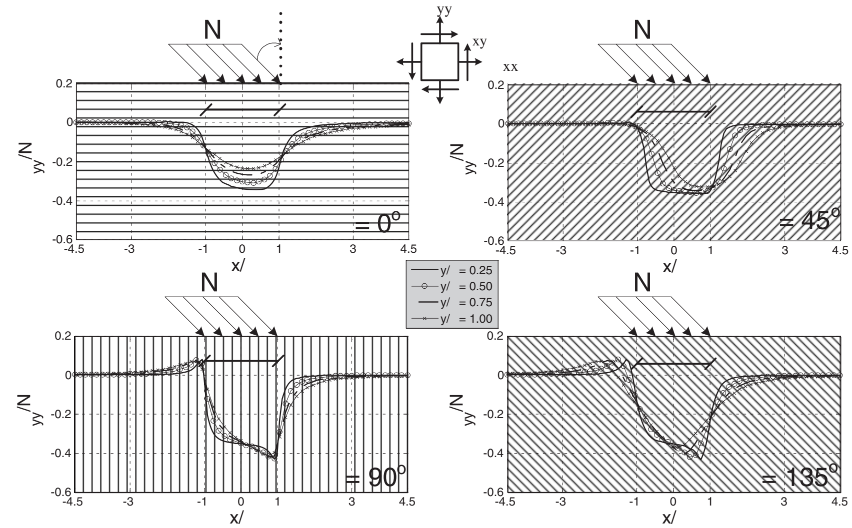

Figure 3: Variation of σ_{yy} due to line load distributions on a width 2ε of 20 μm with respect to x/ε for $\alpha = 45^{\circ}$.

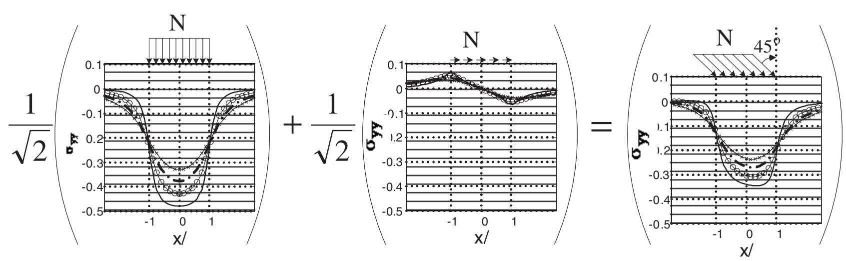

Figure 4: Stresses acting in fiber-orientation $\theta = 0^{\circ}$ due to combination load have been demonstrated as a sum of stresses due to normal and tangential load cases since the stress-field generation lies in the purview of linear elasticity.

Both compressive and tensile stresses are in play although the magnitude of tensile stress is very small for 45° laminate. The $45^{\circ}/135^{\circ}$ laminate stress fields cease to be mirror images due to the additive stress effects.

Finally, Figure 6 depicts the evolution of τ_{xy} distribution for the combined load case. Most FRPs have a lower shear strength values as compared with tensile or compressive strengths in parallel/perpendicular fiber directions. Therefore, the magnitude of τ_{xy} is of great importance in ascertaining the failure behavior of a given FRP laminate which will be dealt with in subsequent works.

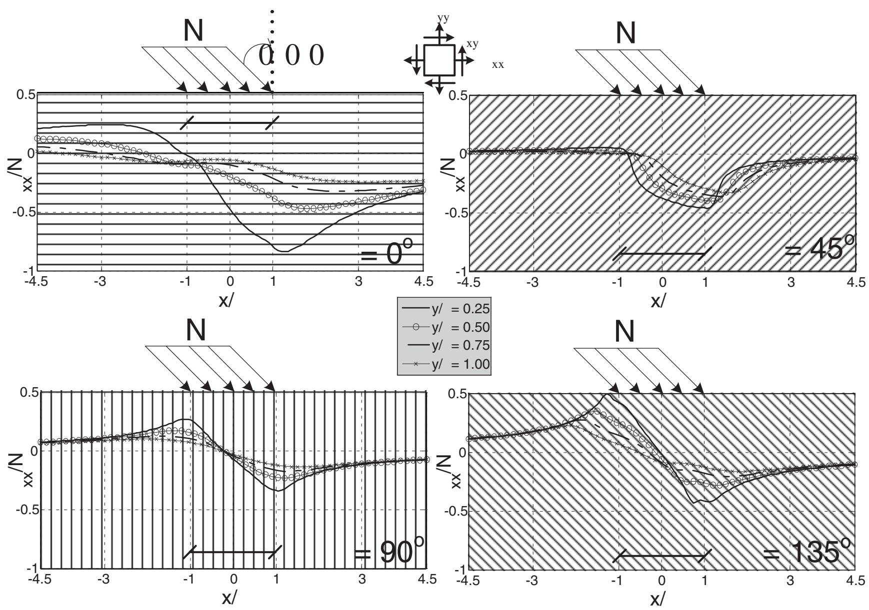

Figure 5: Variation of σ_{xx} due to line load distributions on a width 2ε of 20 µm with respect to x/ε for Combination Case ($\alpha = 45^{o}$).

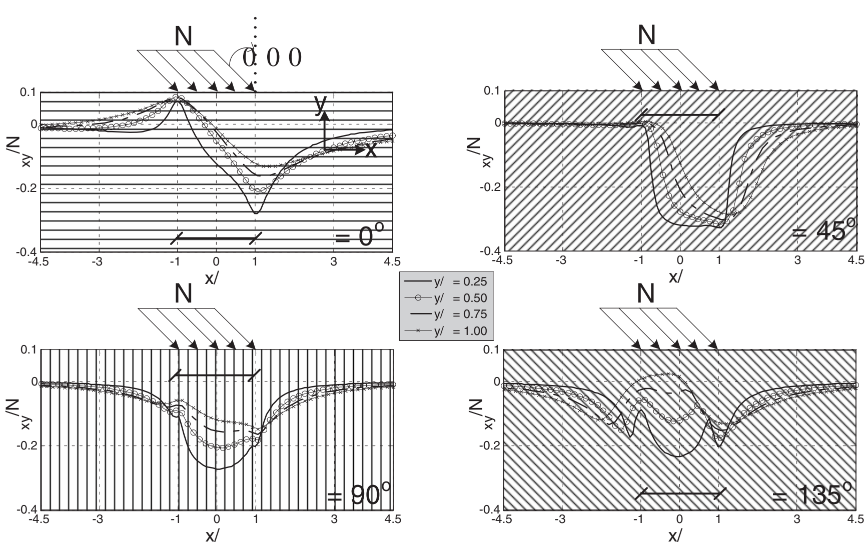

Figure 6: Variation of τ_{xy} due to line load distributions on a width 2ε of 20 µm with respect to x/ε for Combination Load Case ($\alpha = 45^{o}$).

Conclusions and Future work

The basic idea behind this investigation has been to observe and compare the corresponding stress fields in different fiber orientations due to a constant applied line load. The variation in the stress fields among the various fiber-orientations results due to the anisotropic nature of the half-space under consideration. The relation of stress-fields to failure needs to be looked into in future. And finally, the applicability of the present problem to edge-trimming process in UD-FRP laminates needs to be addressed.

References

1 Gururaja, S. and Ramulu, M. (Submitted for publication on Sep, 2006): “Stress analysis of fibrous composites as an anisotropic half-space”, *Mechanics Research Communication.*

2 Lekhnitskii, S. G. (1977): *Theory of elasticity of an anisotropic body,* Moscow: Mir Publishers.

3 Muskhelishvelli, N. (1953): *Some basic problem of the mathematical theory of elasticity; fundamental equations, plane theory of elasticity, torsion and bending,* Moscow: 5th Edition, Nauka.

4 Ning, X. and Lovell, M. R. (2002): “On the sliding friction characteristics of unidirectional continuous FRP composites”, *Transactions of ASME: Journal of Tribology.* Vol. 124, pp.5 – 13.

5 Ning, X., Lovell, M. R. and Morrow, C. (2004): “Anisotropic strength approach for wear analysis of unidirectional continuous FRP composites”, *Transactions of ASME: Journal of Tribology,* Vol. 126, pp.65 – 70.

6 Liao, J. J. and Wang, C. (1998): “Elastic solutions for a transversely isotropic half-space subjected to a point load”, *International Journal of Numerical and Analytical Methods in Geomechanics,* Vol. 22, pp.425 – 447.

7 Smith, J. O. and Liu, C. K. (1953): “Stresses due to tangential and normal loads on an elastic contact with application to some contact problems”, *Transactions of ASME:Journal of Applied Mechanics*, Vol. 20, pp.157 – 166.